



Pharmaceutics, Drug Delivery and Pharmaceutical Technology

Surface Tracking of Curcumin Amorphous Solid Dispersions Formulated by Binary Polymers

Na Fan^b, Tong Lu^a, Jing Li^{a,*}^a School of Basic Medical Science, Shenyang Medical College, Shenyang, Liaoning, China^b Wuya College of Innovation, Shenyang Pharmaceutical University, Shenyang, Liaoning, China

ARTICLE INFO

Article history:

Received 5 August 2019

Revised 13 September 2019

Accepted 15 October 2019

Available online 19 October 2019

Keywords:

hydroxypropyl methylcellulose
amorphous solid dispersions
tautomeric curcumin
binary polymers

ABSTRACT

Herein, curcumin amorphous solid dispersions (Cur ASDs) were prepared using binary polymers (Eudragit EPO with polyvinylpyrrolidone K30 [EuD-PVP], Eudragit EPO with hydroxypropyl methylcellulose E50 [EuD-HPMC]) as excipient, and surface tracking of Cur ASDs was mainly addressed. Infrared spectroscopy, *in situ* Raman imaging spectroscopy, molecular docking modeling, and contact angle measurements were mainly applied to study the molecular interaction and wetting property of Cur ASDs. Cur/EuD-PVP had a lower cumulative release (approximately 15%) than Cur/EuD-HPMC (approximately 48%) because Cur/EuD-HPMC presented carrier-controlled wetting property while Cur/EuD-PVP fitted to a drug-controlled wetting property. The favorable HPMC can be preferred as superior excipient for Cur ASDs compared with binary polymers, which has potential application in food and drug healthcare industry of Cur.

© 2020 American Pharmacists Association®. Published by Elsevier Inc. All rights reserved.

Introduction

It is well known that curcumin (Cur), which has a keto form and enol form, is a hydrophobic polyphenol derived from the rhizome of turmeric (*Curcuma longa*) and has been widely used as a nutritional supplement in many Asian countries for thousands of years.¹ In the current stage, Cur has received great attention for its beneficial applications in anti-oxidant, anti-cancer, and anti-inflammatory effects.²⁻⁴ According to experiments, Cur has a significant effect on acute and chronic gastric ulcer models in rats. Cur prevented gastric mucosal lesions in a dose-dependent manner and enhanced the healing of chronic gastric ulcer curative efficacy. It has reported that Cur can be daily administered 12 g, and there is no toxicity to take 8 g Cur for 3 months.^{1,5} Unexpectedly, the poor dissolution and oral bioavailability of Cur have been thoroughly demonstrated in both animals and humans, largely due to factors including poor aqueous solubility, chemical instability, and metabolic susceptibility. Cur degrades quickly in neutral or alkaline buffer solution, which also limits its usage.⁶ Therefore, formulation

techniques or drug delivery systems with the abilities to increase the solubility and stability of Cur are important targets to enable its uses for enhancing human health.

Various formulation approaches have been made to design Cur formulations, including liposomes, nanoparticles, amorphous solid dispersions (ASDs),⁵ self-emulsifying drug delivery systems, and cyclodextrin complexation.⁷ Various hydrophilic polymers such as polyoxyethylene pyrrolidone K30, polyethylene glycol 4000 and polyethylene glycol 6000, and Eudragit EPO (EuD) have been tested for dissolution rate enhancement of Cur by different solid dispersion techniques.^{2,8-10} It should be noted that EuD, with a maximum solubility in gastric fluids up to pH 5, is a cationic polyelectrolyte that belongs to the family of (meth)acrylate copolymers.¹¹ As EuD has positive charges, negatively charged drugs including Cur can be selected as a model drug and incorporated into ASDs. EuD can be used as a superior carrier for Cur ASDs, owing to its advantages, including good taste masking, moisture-proof character, and gastric solubility (Fig. 1).^{2,11} Although there are several reports on Cur ASDs, it is also not understood how different structural forms (keto or enol) of Cur interact with binary polymers in ASDs.

In the process of research work, we found that Cur-loaded binary polymers (Cur/EuD-PVP [polyvinylpyrrolidone K30], Cur/EuD-HPMC [hydroxypropyl methylcellulose E50]) showed opposite dissolution performance compared to Cur/EuD. To clearly elucidate the reason for this difference, the current study focuses on intermolecular interaction between Cur and binary polymers as well as

Conflict of interest: There is no conflict of interest in this paper. It does not involve informed consent or animal studies.

This article contains supplementary material available from the authors by request or via the Internet at <https://doi.org/10.1016/j.xphs.2019.10.030>.

* Correspondence to: Jing Li (Telephone: +86-024-62215759).

E-mail address: dddefghijklmn@163.com (J. Li).

the wetting property of as-synthesized Cur ASDs.¹² Tautomeric Cur in ASDs was probed to vividly demonstrate their existence and specifically reveal molecular interactions between the keto and enol forms of Cur with binary polymers to determine the vital molecular forces that contribute to the interaction between polymers and Cur. The great novelty of this paper is to clearly elucidate the surface science of Cur ASDs formulated by EuD as main excipient.

Materials and Methods

Materials

Cur with purity above 99.8% was purchased from Meilunbio Company, Ltd. (Dalian, China). HPMC and PVP were obtained from Anhui Shanhe Pharmaceutical Excipients Company, Ltd. (Huainan, China). EuD was kindly provided by Evonik Company, Ltd. (Essen, Germany). Other chemical agents were obtained from Tianjin Bodi Chemical Holding Company, Ltd. (Tianjin, China).

Preparation of Cur ASDs

EuD or binary polymers (EuD-PVP, EuD-HPMC) were dissolved in a small amount of ethanol. In the meantime, Cur was completely dissolved in ethanol (about 20 mL) in an 80°C water bath. The weight ratio between the carrier and drug was designed as 4:1. The above solution was mixed, and ethanol was removed by rotary evaporation. The ASDs were then dried in a vacuum oven overnight to remove residual solvent. The ASDs were sieved to obtain uniform particles and finally stored in a desiccator containing phosphorus pentoxide at room temperature.

Molecular Interaction

IR

IR (Spectrum 1000; PerkinElmer, Waltham, MA) spectra of samples were obtained over the spectral region 400–4000/cm. Samples were prepared by gently and respectively grinding drug, excipient, and ASDs with KBr.

Raman Spectroscopy

The solid state of sample surface was analyzed *in situ* through a quartz sight window using a Raman spectrometer (inVia Laser Micro Raman Spectroscopy; Renishaw PLC, Gloucestershire, UK). The measurements were conducted with a 500 mW laser source at a wavelength of 785 nm.

Molecular Docking Modeling

The keto and enol forms of Cur were drawn using Marvin sketch software. The 3-dimensional structures of macromolecules (HPMC, PVP, EuD) were created by optimizing the structural minimization and the structural dynamics using the Sybyl 6.9.1 software package (Tripos Associates, St. Louis, MO, 2003). The optimization parameters consist of Energy Change 0.005 (kcal/mol) and Max Iterations 10,000. All other parameters were maintained at the default values. The complexes between Cur and polymers were studied using molecular docking via AutoDock 4.0 software.¹³

XRD

The samples were analyzed using a Shimadzu X-ray diffraction (XRD)-6000 diffractometer (Shimadzu Corporation, Kyoto, Japan) equipped with a Cu-K α source and set in Bragg-Brentano geometry, scanning between 5°C and 40°C 2 θ at 8°C/min with a 0.04° step size.

In Vitro Dissolution

Drug release experiments were performed using USP II method (50 rpm, 37°C) with an RC806D dissolution tester (Tianjin, China). Cur ASDs were exposed to enzyme-free simulated gastric fluid (pH 1.0 hydrochloric acid). At predetermined time intervals, 5 mL samples were withdrawn from the release medium and an equivalent amount of fresh medium was added to maintain a constant dissolution volume. Samples administered through a 0.45- μ m microporous membrane were analyzed using an UV-1120 instrument (Shimadzu, Japan) at 425 nm. The UV scanning image of Cur is present in the [Supporting Information](#).

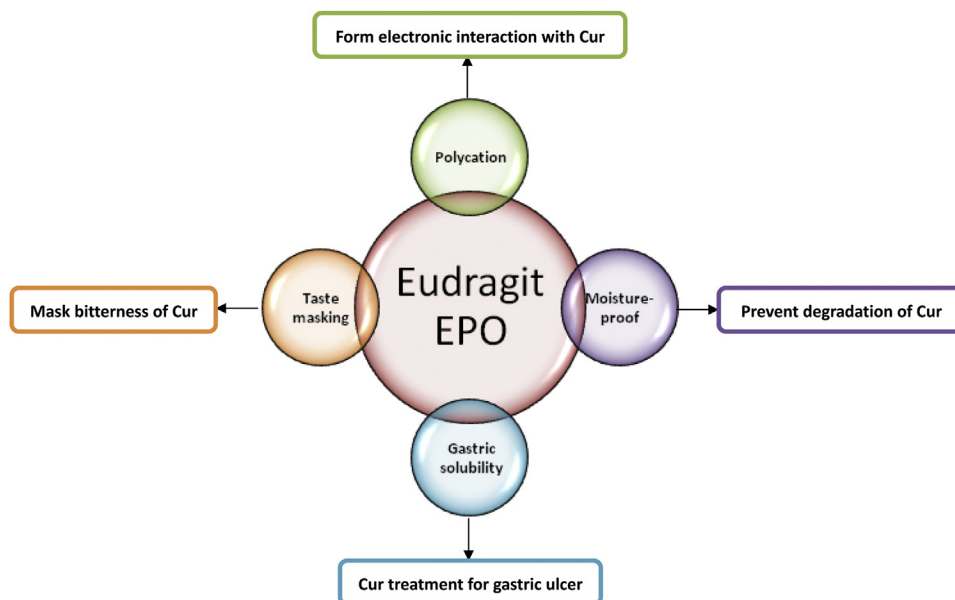


Figure 1. Brief summary of the advantages for applying EuD as Cur carrier.

In Vitro Solubility and Permeability

Cur solubility under physiological pH environment was conducted. Excess amount of crystalline Cur was added to a certain amount of pH 1.0 hydrochloric acid. The system was agitated for 48 h at 37°C. The supernatant was then separated by centrifugation

and drug concentration was measured using HPLC method. The working conditions included a Kromasil (C₁₈) 150 × 4.6 mm, 428 nm UV visible detector, and the mobile phase consisted of methanol:water:ice acetic acid (77:22:1, v/v/v).

Cur permeability was studied using *in vitro* permeability test. Briefly, phospholipid solution was spread onto the

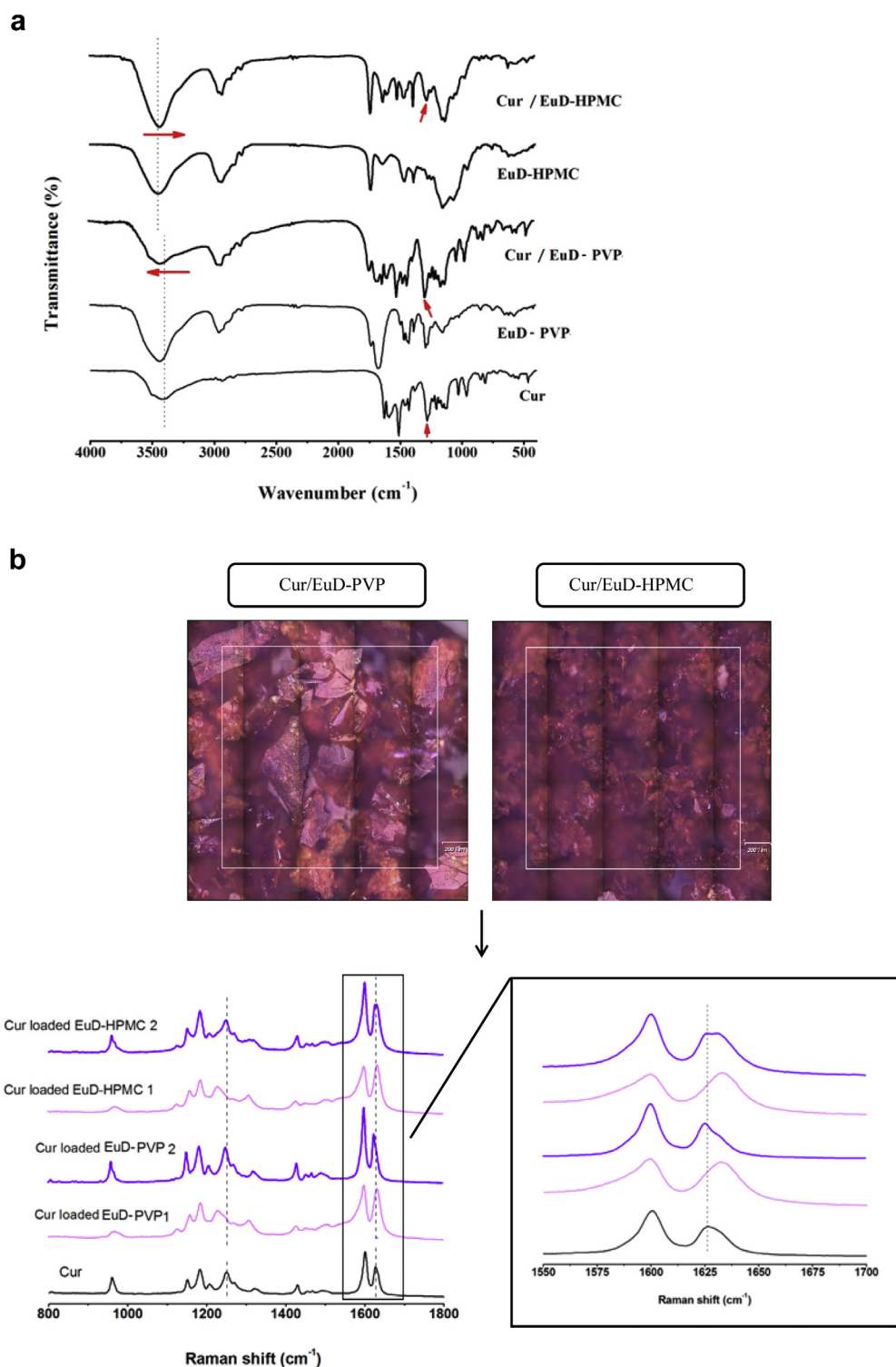


Figure 2. (a) IR spectra of Cur, EuD-PVP, Cur/EuD-PVP, EuD-HPMC, Cur/EuD-HPMC. (b) Raman image and spectroscopy of several samples. (c) Molecular docking images of tautomeric Cur with excipient. (d) Molecular docking result of Cur with excipient.

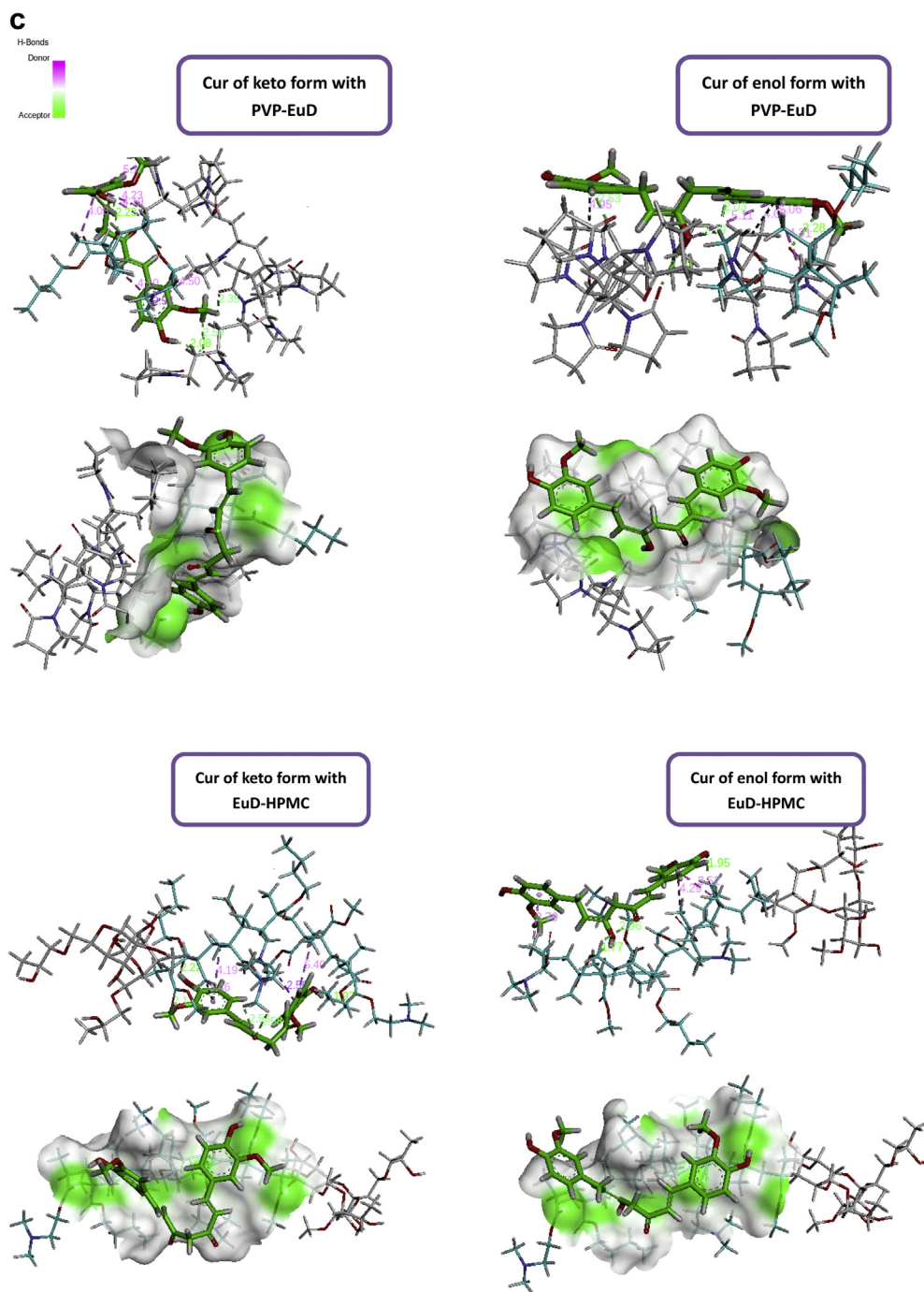


Figure 2. (continued).

microfiltration membrane and inserted between diffusion cells. Samples containing 4 mg Cur was put in the above supply chamber and the receiving chamber contained pH 1.0 hydrochloric acid solution. One hundred microliter medium in receiver compartment was withdrawn at 48 h and measured drug concentration.

Contact Angle Measurement

As an important index of wettability, contact angles were measured to study interfacial wetting behavior. The contact angle of samples was measured using the operation manual for an

automatic contact angle meter model JCY series (Shanghai, China). Briefly, 200 mg Cur, excipient, or Cur ASDs was weighed and compressed under pressure of 10^9 Pa. A drop of enzyme-free simulated gastric fluid (2 μ L) was placed on the compressed plate and the initial contact angle was measured.¹⁴

Inverted Fluorescence Microscope

To vividly present and confirm the wetting behavior of Cur ASDs, inverted fluorescence microscope (Olympus, Japan) was applied for observing sample powder with or without one drop of dissolution medium. The magnification was set at 10×10 times.

d

	Name	Visible	Color	Parent	Distance	Category	Types
1	d:<1>0...	<input checked="" type="checkbox"/> Yes	■	Ligand ...	2.08495	Hydrogen Bond	Conventional Hydrogen Bond
2	d:<1>0...	<input checked="" type="checkbox"/> Yes	■	Ligand ...	2.22794	Hydrogen Bond	Conventional Hydrogen Bond
3	d:<1>0...	<input checked="" type="checkbox"/> Yes	■	Ligand ...	2.34805	Hydrogen Bond	Carbon Hydrogen Bond
4	d:<1>0...	<input checked="" type="checkbox"/> Yes	■	Ligand ...	2.58932	Hydrogen Bond	Carbon Hydrogen Bond
5	:UNK1:...	<input checked="" type="checkbox"/> Yes	■	Ligand ...	2.53568	Hydrophobic	Pi-Sigma
6	d:<1>0...	<input checked="" type="checkbox"/> Yes	■	Ligand ...	4.49831	Hydrophobic	Pi-Alkyl
7	d:<1>0...	<input checked="" type="checkbox"/> Yes	■	Ligand ...	4.09708	Hydrophobic	Pi-Alkyl
8	d:<1>0...	<input checked="" type="checkbox"/> Yes	■	Ligand ...	5.14218	Hydrophobic	Pi-Alkyl
9	d:<1>0...	<input checked="" type="checkbox"/> Yes	■	Ligand ...	4.18902	Hydrophobic	Pi-Alkyl
10	d:<1>0...	<input checked="" type="checkbox"/> Yes	■	Ligand ...	4.08282	Hydrophobic	Pi-Alkyl
11	d:<1>0...	<input checked="" type="checkbox"/> Yes	■	Ligand ...	4.226	Hydrophobic	Pi-Alkyl

Molecular docking result of Cur of keto form with EuD-PVP

	Name	Visible	Color	Parent	Distance	Category	Types
1	d:<1>0...	<input checked="" type="checkbox"/> Yes	■	Ligand ...	2.13072	Hydrogen Bond	Conventional Hydrogen Bond
2	d:<1>0...	<input checked="" type="checkbox"/> Yes	■	Ligand ...	2.27869	Hydrogen Bond	Conventional Hydrogen Bond
3	:UNK1:...	<input checked="" type="checkbox"/> Yes	■	Ligand ...	2.53342	Hydrogen Bond	Carbon Hydrogen Bond
4	:UNK1:...	<input checked="" type="checkbox"/> Yes	■	Ligand ...	2.29241	Hydrogen Bond	Carbon Hydrogen Bond
5	:UNK1:...	<input checked="" type="checkbox"/> Yes	■	Ligand ...	2.03009	Hydrogen Bond	Carbon Hydrogen Bond
6	d:<1>0...	<input checked="" type="checkbox"/> Yes	■	Ligand ...	4.95134	Hydrophobic	Pi-Alkyl
7	d:<1>0...	<input checked="" type="checkbox"/> Yes	■	Ligand ...	5.10571	Hydrophobic	Pi-Alkyl
8	d:<1>0...	<input checked="" type="checkbox"/> Yes	■	Ligand ...	4.6818	Hydrophobic	Pi-Alkyl
9	d:<1>0...	<input checked="" type="checkbox"/> Yes	■	Ligand ...	5.0565	Hydrophobic	Pi-Alkyl
10	d:<1>0...	<input checked="" type="checkbox"/> Yes	■	Ligand ...	4.31478	Hydrophobic	Pi-Alkyl

Molecular docking result of Cur of enol form with EuD-PVP

	Name	Visible	Color	Parent	Distance	Category	Types
1	d:RES1:...	<input checked="" type="checkbox"/> Yes	■	Ligand ...	1.76587	Hydrogen Bond	Conventional Hydrogen Bond
2	d:RES1:...	<input checked="" type="checkbox"/> Yes	■	Ligand ...	1.95044	Hydrogen Bond	Conventional Hydrogen Bond
3	:UNK1:...	<input checked="" type="checkbox"/> Yes	■	Ligand ...	2.95697	Hydrogen Bond	Carbon Hydrogen Bond
4	d:RES1 ...	<input checked="" type="checkbox"/> Yes	■	Ligand ...	3.79021	Hydrophobic	Pi-Alkyl
5	d:RES1 ...	<input checked="" type="checkbox"/> Yes	■	Ligand ...	4.29414	Hydrophobic	Pi-Alkyl
6	d:RES1 ...	<input checked="" type="checkbox"/> Yes	■	Ligand ...	3.52129	Hydrophobic	Pi-Alkyl

Molecular docking result of Cur of keto form with EuD-HPMC

	Name	Visible	Color	Parent	Distance	Category	Types
1	d:<1>0...	<input checked="" type="checkbox"/> Yes	■	Ligand ...	2.21538	Hydrogen Bond	Conventional Hydrogen Bond
2	d:<1>0...	<input checked="" type="checkbox"/> Yes	■	Ligand ...	1.96985	Hydrogen Bond	Conventional Hydrogen Bond
3	:UNK1:...	<input checked="" type="checkbox"/> Yes	■	Ligand ...	2.5275	Hydrogen Bond	Carbon Hydrogen Bond
4	:UNK1:...	<input checked="" type="checkbox"/> Yes	■	Ligand ...	2.57636	Hydrogen Bond	Carbon Hydrogen Bond
5	d:<1>0...	<input checked="" type="checkbox"/> Yes	■	Ligand ...	2.13218	Hydrogen Bond	Carbon Hydrogen Bond
6	:UNK1:...	<input checked="" type="checkbox"/> Yes	■	Ligand ...	2.55594	Hydrophobic	Pi-Sigma
7	d:<1>0...	<input checked="" type="checkbox"/> Yes	■	Ligand ...	4.1869	Hydrophobic	Pi-Alkyl
8	d:<1>0...	<input checked="" type="checkbox"/> Yes	■	Ligand ...	3.46448	Hydrophobic	Pi-Alkyl
9	d:<1>0...	<input checked="" type="checkbox"/> Yes	■	Ligand ...	5.396	Hydrophobic	Pi-Alkyl

Molecular docking result of Cur of enol form with EuD-HPMC

Figure 2. (continued).

Results and Discussion

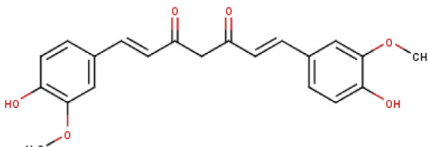
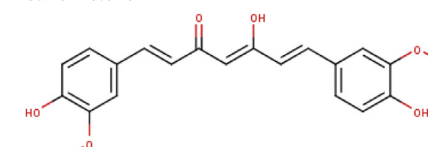
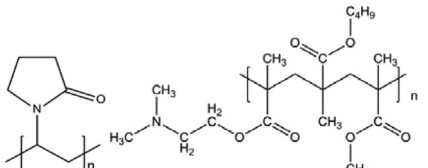
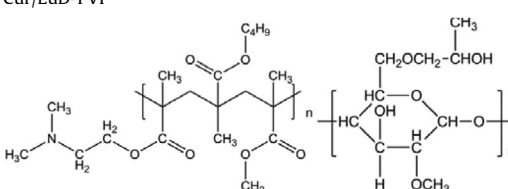
Molecular Interaction

IR

The possible interaction between Cur and binary polymers was studied through IR analysis. The IR spectra of Cur, a mixed

polymer combination, and Cur ASDs are presented in Figure 2a and specific data are shown in Table 1. The –OH stretch peak at 3418/cm in Cur showed obvious differences, demonstrating that phenol OH group and OH from the enol form of Cur interacted with the carrier. Moreover, the bending vibration of –OH in Cur confirmed that the main group that formed interactions with excipient in ASDs was the phenol –OH group. In IR analysis

Table 1
IR Information of Cur, Excipient, and Cur ASDs

Sample	Main Peak (/cm)	Stretch of C=O (EuD) (/cm)	Other Peaks (/cm)	Banding Vibration of OH (Cur) (/cm)
 Cur of keto form	3418	—	1627 (Cur)	1282
 Cur of enol form				
 EuD-PVP Cur/EuD-PVP	3438	1668	—	—
 EuD-HPMC Cur/EuD-HPMC	3422	1732	1673 (PVP)	1283
	3440	1730	1631 (HPMC)	—
	3428	1729	1628 (Cur)	1272

of the binary polymer and its corresponding ASDs, initial consideration should be paid to the large peak from 3300 to 3500/cm. The shift in Cur ASD peaks for polymer or Cur can be determined based on peak morphology and intensity. If the peak morphology and intensity was close to the IR spectrum of mixed polymers, the peak shift should be compared to Cur ASDs and mixed polymers, not Cur ASDs and Cur. Therefore, the main peak of Cur/EuD-PVP was ascribed to the Cur spectrum, while that of Cur/EuD-HPMC belonged to the spectrum of mixed polymers. In detail, for the mixture of EuD-PVP, the stretches for C–O and C=O can be observed at 3438 and 1668/cm, respectively. After forming Cur ASDs, the 2 polymers and Cur shifted to higher wavenumbers, suggesting that hydrogen bond interactions were generated. The results also demonstrated that the formation of hydrogen bonds involved the carbonyl group in EuD-PVP that accepted the H atom from the –OH group of Cur because the C=O stretch from Cur (1627/cm) did not show a large peak shift in Cur/EuD-PVP. For the mixture of EuD-HPMC, all components shifted to much lower wavenumbers, and thus the shift was stronger for EuD-PVP, hinting that stronger hydrogen bonds were formed in Cur/EuD-HPMC relative to Cur/EuD-PVP. Apart from the carbonyl group in the EuD that accepted the H atom from the –OH group of Cur, the C=O in Cur also contributed the hydrogen bond because the stretch of C=O from Cur (1627/cm) disappeared in Cur/EuD-HPMC, illustrating that the –OH group in HPMC can form hydrogen bonds with the C=O group from Cur.

Raman Imaging Spectroscopy

In addition to IR, Raman spectroscopy (Fig. 2b) can facilitate analysis of molecular interactions between drugs and carriers in terms of non-polar bonds,¹⁵ providing valuable information on different levels of molecular interactions for the 2 forms of Cur. According to the *in situ* Raman images, Cur/EuD-PVP and Cur/EuD-HPMC presented 2 types of Raman spectra. Because the Raman signal of Cur was almost 10^3 stronger than any excipient used, the Raman spectrum reflected the existing state of Cur in ASDs. As illustrated in our previous work,¹⁶ it was clear that the signal of Raman image and spectrum belonged to Cur because the Raman signal of Cur was almost 10^3 stronger than any excipient used. The spectrum of Cur sample was keto form when its spectrum was similar to the spectrum of Cur, and the spectrum of Cur sample was keto form when it presented co-shift of –OH group at around 1270/cm and carbonyl group at around 1627/cm. Therefore, the observed 2 types of Raman spectra can be ascribed to the Cur keto form and the Cur enol form. Several important conclusions can be drawn from the Raman spectra, including (1) the –OH of Cur near 1250/cm and carbonyl group near 1627/cm for Cur ASDs (Cur/EuD-PVP 1 [the first Cur form in Cur/EuD-PVP] and Cur/EuD-HPMC 1 [the first Cur form in Cur/EuD-HPMC]) shifted to lower and higher wavenumbers compared to Cur, suggesting that the –OH group and carbonyl group from the Cur enol form were present in these samples and that the first Cur form was enol form. In this principle, the Cur keto form contributed to Cur/EuD-PVP 2 as well as Cur/EuD-HPMC 2; (2) the

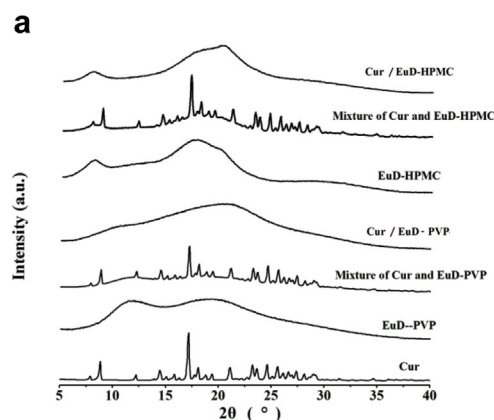
Raman signals of Cur/EuD-PVP 1 and Cur/EuD-HPMC 1 were significantly lower than Cur/EuD-PVP 2 and Cur/EuD-HPMC 2, which may hint that the Cur keto form formed stronger interactions with polymers; (3) based on the findings above, the molecular interaction (mainly hydrogen bond forces) of Cur/EuD-PVP was predicted to be lower than Cur/EuD-HPMC because there was more Cur enol form in the former ASDs.

Molecular Docking Modeling

To reveal the molecular interactions between tautomeric Cur and combined polymers, molecular docking techniques were applied. During optimization, the linear structures of the polymers started to bend and finally transformed into coils. The obtained optimized results for complexes presumably represent the most stable polymeric conformations, that is, the lowest total energy.^{17,18} Figures 2c and 2d depict the 3-dimensional molecular docking results of tautomeric Cur with polymers showing interaction distances or the distribution of hydrogen bonds on the inter-surface. The optimized molecular dockings of Cur with keto form and Cur of enol form were obviously different. EuD-PVP and EuD-HPMC showed 2 types of Raman spectra owing to the co-existence of Cur keto and enol forms in ASDs. It was obvious that Cur of enol form can form more hydrogen bonds with excipient compared to Cur of keto form. When comparing the hydrogen bond ratio of Cur with keto form and enol forms, Cur with EuD-PVP had a lower hydrogen bond ratio (4/9) originating from the Cur of the keto form, demonstrating lower hydrogen bond forces than for Cur with EuD-HPMC (1/2), which was in agreement with previous IR result. The clear probing of tautomeric Cur with binary polymers, mainly by Raman and molecular modeling techniques, leads us to comprehend Cur ASDs at the molecular level.

XRD

The X-ray diffraction patterns of Cur, excipient, physical mixtures, and Cur ASDs are shown in Figure 3a. Cur was in crystal state evidenced by a series of characteristic peaks (7.89°, 8.82°, 12.22°, 14.45°, 17.15°, 21.13°, 24.65°, and 29.09° 2θ). There are 3 kinds of Cur polymorphs based on the report. Herein, Cur belonged to Form 1 according to XRD result. The XRD patterns of all physical mixtures showed the characteristic peaks that are similar to crystalline Cur, indicating the presence of crystalline Cur in the physical mixtures.^{19,20} The result showed that Cur/EuD-PVP as well as Cur/EuD-HPMC did not display any drug peaks, demonstrating that amorphous Cur remained in these Cur ASDs.



Drug Dissolution

To clearly present the function of each excipient in Cur ASDs, the *in vitro* drug dissolution profile of Cur and Cur/EuD was provided apart from Cur/EuD-PVP and Cur/EuD-HPMC (see Fig. 3b). Several key points addressed by the results included the following: (1) compared to pure Cur, all Cur ASDs enhanced drug dissolution due to amorphous Cur distributed in the matrix of the ASDs^{21,22}; (2) because the higher weight ratio of excipient in polymer combinations was considered as the main functional carrier in Cur ASDs, Cur/EuD-PVP that was primarily monitored by a diffusion mechanism had lower cumulative release (approximately 15%) than Cur/EuD-HPMC (approximately 48%), which was controlled by an erosion mechanism; and (3) the highest cumulative release of Cur/EuD-PVP was lower than Cur/EuD while Cur/EuD-HPMC was better than Cur/EuD; the following wetting property study of contact angle measurement and inverted fluorescence microscope can provide sufficient explanation.

Drug Solubility and Permeability

Figure 4a shows the Cur concentration of Cur, Cur/EuD-PVP, and Cur/EuD-HPMC. It was obvious that solid dispersion strategy can significantly improve Cur concentration in pH 1.0 hydrochloric acid. The enhanced level of Cur concentration was mainly attributed to the fact that EuD was able to form ionic interactions with Cur. The ionic interaction of EuD and Cur was stronger than the intermolecular hydrogen bonds of Cur-Cur, thus providing enhanced energy to depart Cur-Cur and disperse drug molecules into the medium. Compared with EuD-PVP, EuD-HPMC had superiority in enhancing Cur solubility, which can be explained in the following contact angle measurement discussion.

In vitro transmembrane result (Fig. 4b) confirmed the ability of Cur/EuD-PVP and Cur/EuD-HPMC in improving Cur permeability owing to the enhancement of Cur solubility. It should be noted that HPMC had effective ability in enhancing drug permeability because its transmembrane improvement was much higher than the enhancement of Cur solubility. The reason was because HPMC molecule chains were charged under acidic medium that simulate gastric fluid. These charged molecular chains tended to extend, thus reducing the surface tension formed between hydrophobic groups of HPMC and phospholipids on the outside layer. Therefore, the un-ordered state of phospholipids lead to the enhancement of Cur transmembrane using HPMC as auxiliary excipient, which contributed greatly to the Cur permeability.

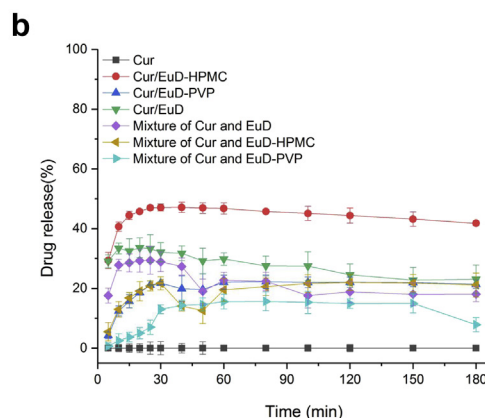


Figure 3. (a) XRD of Cur, excipient, physical mixture, and Cur ASDs. (b) *In vitro* dissolution of Cur, Cur/EuD-PVP, Cur/EuD, Cur/EuD-HPMC, and their physical mixtures.

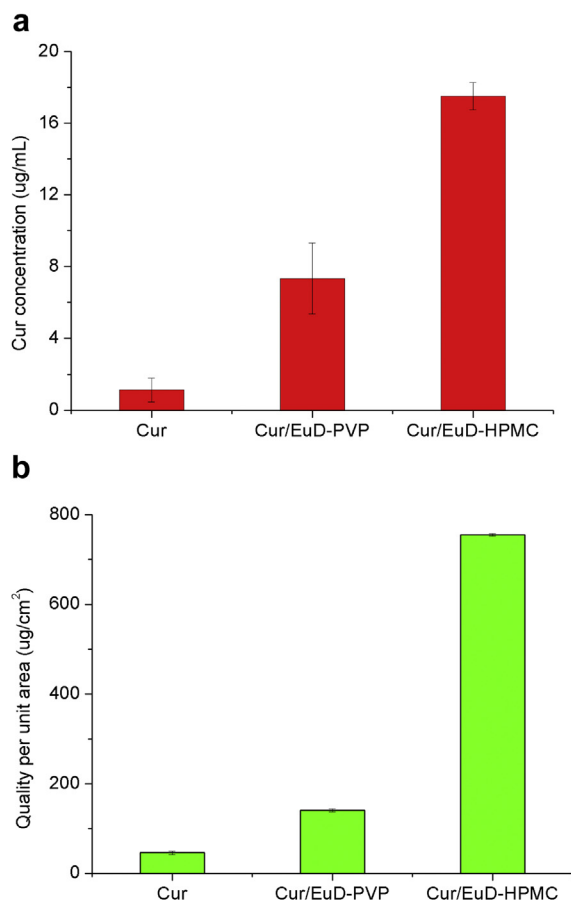


Figure 4. (a) Cur solubility of Cur, Cur/EuD-PVP, and Cur/EuD-HPMC. (b) *In vitro* permeability of Cur, Cur/EuD-PVP, and Cur/EuD-HPMC.

Wetting Property

Wetting property of ASDs is crucial for comprehending *in vitro* dissolution process. A series of water contact angle measurements aiming to reflect the wetting property of Cur ASDs were performed on Cur ASD tablets and tablets compacted from pure excipient, a physical mixture of excipient and drug, or pure drugs. Compared to Cur/EuD-PVP, the contact angle of Cur/EuD-HPMC was obviously lower, and both the solid adhesion and surface-free energy of Cur/EuD-HPMC showed significantly higher values, suggesting that Cur/EuD-HPMC with stronger molecular interaction forces than Cur/EuD-PVP had higher energy to display better wetting properties. The superior wetting property can be a foundation for the higher Cur dissolution of Cur/EuD-HPMC compared to Cur/EuD-PVP. Although this is not sufficient for the presented discussion and conclusions, the in-depth analysis can be presented after managing the data, primarily through trend fittings and comparing data for excipients and physical mixtures with Cur ASDs.

As shown in Figure 5, the contact angle of EuD-PVP fitted well with the logarithmic function equation, while the physical mixture of drugs with excipient together with Cur/EuD-PVP were best accorded with a binomial function. Because the fitted equation of the contact angle of Cur was a binomial function ($y = 0.0005x^2 - 0.2371x + 72.976$), the contact angle analysis of Cur/EuD-PVP demonstrated that the determined factor for controlling the wetting property of Cur/EuD-PVP was Cur, not the excipient. In contrast, the contact angle of both excipient (EuD-HPMC) and Cur ASDs (Cur/EuD-HPMC) was suitable for a power function equation

but not for the physical mixture of drug with excipient, showing that excipient dominated the wetting behavior of Cur/EuD-HPMC. These interesting and important results indicate that the wetting behavior of Cur ASDs differed when applied to different polymer combinations as a carrier.

The scientific value of the profile fitting can be used to explore and facilitate the wetting property of Cur ASDs in the interfacial wetting aspect. It has been widely accepted that the drug dissolution of ASDs can be divided into carrier-controlled and drug-controlled dissolution.²³⁻²⁵ When the drug was dissolved into the polymer-rich diffusion layer at a sufficiently rapid rate, there was insufficient time for drug molecules to be released intact into the medium. In this case, the drug was molecularly dispersed within this concentrated layer, leading to carrier-controlled dissolution. If dissolution into the polymer diffusion layer was comparatively slow, drug released as solid particles and its release will not be associated with the polymer but will instead be dominated by its characteristics (size, physical form, etc.), that is, drug-controlled dissolution. Here, the wetting property, whether carrier-controlled or drug-controlled, can be distinguished by fitting the trend profile of contact angle measurement and making comparisons of the excipient, physical mixture with ASDs. The dissolution of ASDs was controlled by excipient when the ASD tablet and excipient tablet fitted well to the same type of equation. In other words, carrier-controlled drug release was determined by the excipient, and thus the drug released into the medium along with dissolution of excipient. In contrast, the drug dominated when the trend profile of the contact angle of water for the ASD tablet was fitted with the same type of equation as the drug tablet, demonstrating that the drug-controlled dissolution was governed by the drug itself. Therefore, a preliminary judgment could easily be made for the wetting property of ASDs via fitting of the trend profile of contact angle measurement on a series of tablets, which was certainly important for comprehending the dissolution process and the mechanism of the ASDs.

Based on the above findings, we can conclude that the dissolution of Cur/EuD-PVP followed a drug-controlled wetting property while Cur/EuD-HPMC exhibited a carrier-controlled wetting property. It has been reported that drug release of ASDs via a carrier-controlled wetting property is superior to ASDs with a drug-controlled wetting property, and our *in vitro* release result confirmed this conclusion because the dissolution of Cur/EuD-HPMC was significantly higher than Cur/EuD-PVP. Thus, the drug solubility increased and wetting can be faster because its release resistance was lower than the release with a barrier of excipient. It should be noted that the different drug release pattern may reflect the wetting property of Cur ASDs. The erosion release pattern may result in a carrier-controlled wetting property, and a diffusion-release pattern can lead to a drug-controlled wetting property. The evidence indicated that Cur/EuD-HPMC with an erosion release pattern operated under a carrier-controlled wetting property and Cur/EuD-PVP with a diffusion release pattern fitted to drug-controlled wetting property, which first revealed the facile relationship between release patterns with the wetting property of ASDs.

We also determined the relationship between the wetting property of ASDs and its crystallization pathway. It is widely accepted that possible crystallization pathways from an amorphous solid during dissolution are a solid matrix pathway and a solution pathway. If the dissolution of the solid matrix is slow, crystallization occurs in the solid matrix. If dissolution of the matrix is rapid, the solid dissolves into solution and forms a supersaturated solution via the solution pathway. Based on the contact angle measurements, it was clear that the Cur/EuD-PVP operated under a drug-controlled wetting property, while Cur/EuD-HPMC operated under a carrier-controlled wetting property. The solid matrix of

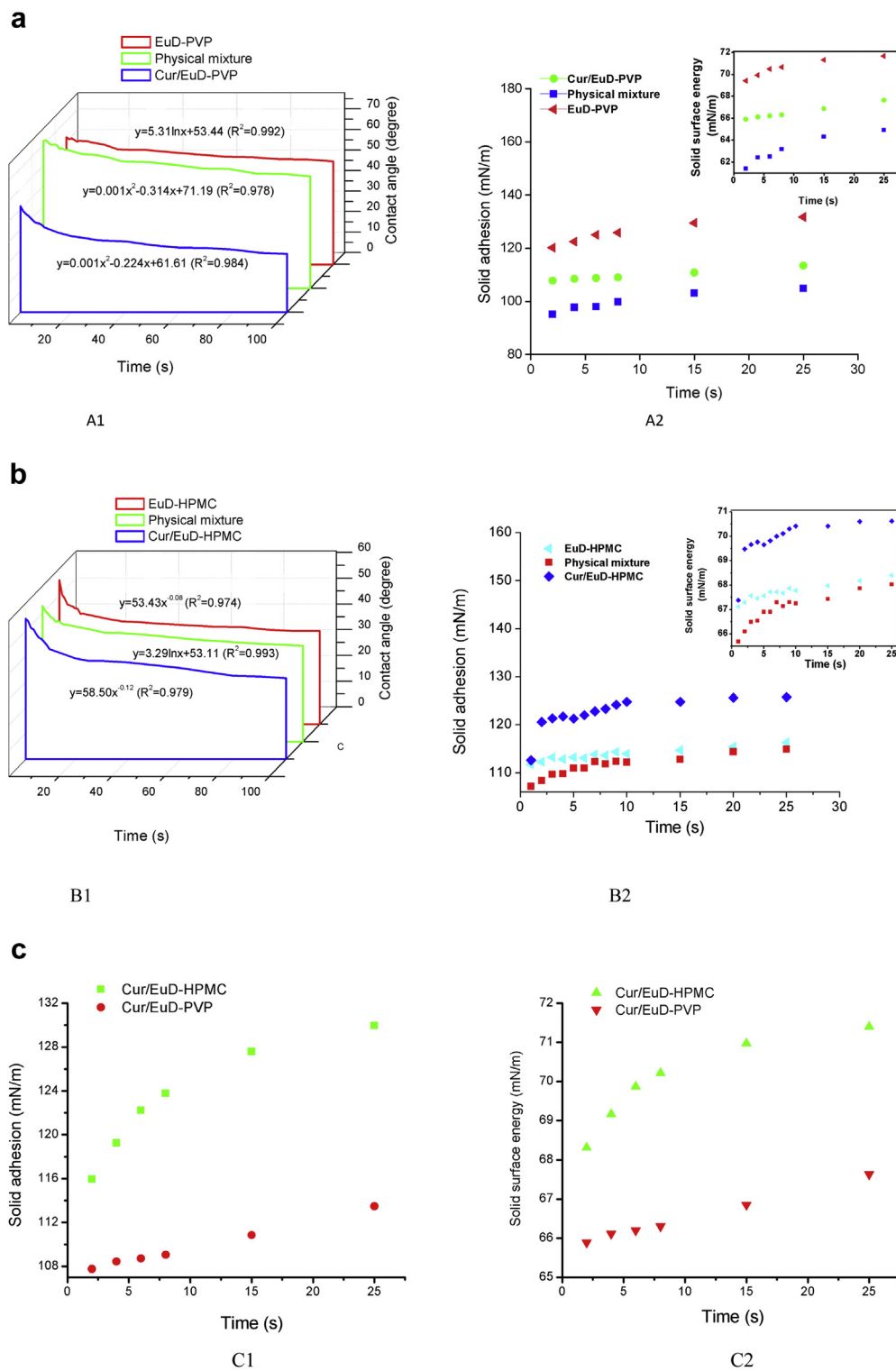


Figure 5. Contact angle measurement results of excipient, physical mixture, and Cur ASDs. A1, contact angle of EuD-PVP, physical mixture, Cur/EuD-PVP; A2, solid adhesion of Cur/EuD-PVP, physical mixture, EuD-PVP; B1, contact angle of EuD-HPMC, physical mixture, Cur/EuD-HPMC; B2, solid adhesion of EuD-HPMC, physical mixture, Cur/EuD-HPMC; C1, solid adhesion of Cur/EuD-HPMC and Cur/EuD-PVP; C2, solid surface energy of Cur/EuD-HPMC and Cur/EuD-PVP.

ASDs under a drug-controlled wetting property dissolves slowly, but dissolves rapidly when ASDs participated in a carrier-controlled wetting property. Thus, Cur/EuD-PVP with a slow dissolution rate of carrier underwent the solid matrix pathway of crystallization, and Cur/EuD-HPMC with a fast dissolution rate of carrier likely

operated under a solution pathway of crystallization, which confirmed the advantage of HPMC in Cur ASDs. From the *in vitro* dissolution results, the reduced concentration of Cur/EuD-HPMC due to crystallization via the solution pathway was obviously more higher than the Cur/EuD-PVP with crystallization of the solid

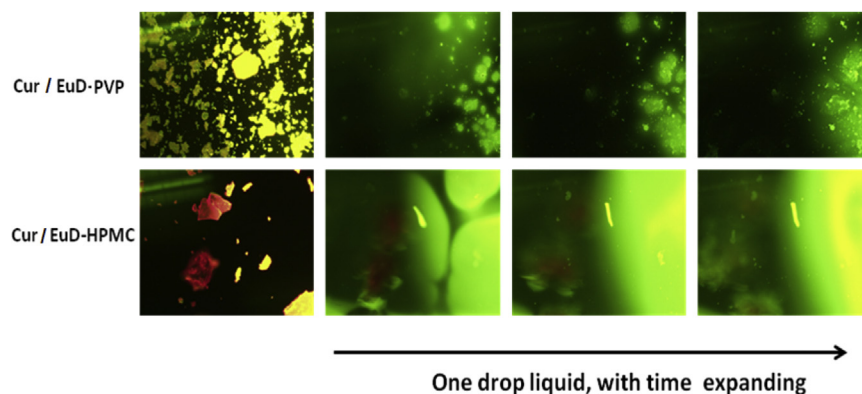


Figure 6. Inverted fluorescence images of Cur/EuD-PVP and Cur/EuD-HPMC with or without one drop of dissolution medium.

matrix pathway, which strongly confirmed that (1) crystallization via a solution pathway was normally faster than the solid matrix pathway reported in the literature and (2) ASDs with a drug-controlled wetting property underwent the solid matrix pathway of crystallization while ASDs with carrier-controlled wetting property belonged to a solution pathway of crystallization. Further study of ASDs focusing on dissolution and crystallization will benefit from this newly discovered elucidation.

Along with the different wetting property for Cur ASDs, the solid adhesion and surface-free energy obtained during contact angle measurements are shown in Figure 5c. The solid adhesion and surface-free energy of excipients (EuD-PVP) were reduced after mixing with Cur because the poorly water-soluble Cur did not contribute energy for wetting. However, the 2 indexes increased for Cur/EuD-PVP compared to the physical mixture, hinting that the interaction forces between amorphous Cur and excipient provided some energy for wetting. It also demonstrated that Cur influenced the solid adhesion and surface-free energy significantly. For Cur/EuD-HPMC, the solid adhesion and surface-free energy did not present significant differences compared to Cur/EuD-PVP, illustrating that Cur did not have an impact on Cur/EuD-HPMC. These results confirmed the wetting property of Cur ASDs described in the present work.

To confirm the wetting property that elucidated using contact angle measurement, inverted fluorescence images of Cur ASDs are presented in Figure 6. It was clear that after dropping one dissolution medium liquid onto Cur/EuD-PVP, excipient was wetted and separated from Cur, resulting in drug-controlled release mechanism. On the contrary, excipient in Cur/EuD-HPMC controlled wetting and release evidenced by the co-erosion phenomenon of Cur/EuD-HPMC. The result confirmed the elucidation of release mechanism that provided in contact angle measurement.

Conclusions

Herein, tautomeric Cur in ASDs formulated with binary polymers (EuD-PVP, EuD-HPMC) was probed using *in situ* Raman imaging spectroscopy and molecular modeling techniques. The wetting property of Cur ASDs was elucidated primarily through contact angle measurements. It was clear that the formation of hydrogen bonds involved the carbonyl group in the PVP and EuD that accepted the H atom from the –OH group of Cur. The molecular interaction (primarily hydrogen bond forces) of Cur/EuD-PVP was lower than Cur/EuD-HPMC due to the larger amount of Cur of the enol form in the former ASDs. Cur/EuD-HPMC with an erosion release pattern belonged to a carrier-controlled wetting property and Cur/EuD-PVP with diffusion release pattern was fitted to a drug-controlled wetting property. For the crystallization pathway, Cur/EuD-PVP with a

slow dissolution rate of carrier underwent the solid matrix pathway of crystallization, and Cur/EuD-HPMC with a fast dissolution rate of carrier likely experienced the solution pathway of crystallization. Therefore, both the elucidation of tautomeric Cur in ASDs at the intermolecular level and its wetting property primarily cover the dissolution and crystallization pathway, reframing our knowledge of Cur ASDs. Furthermore, HPMC can be preferred as superior assistant excipient for Cur ASDs, which has potential application in food and drug healthcare industry of Cur.

References

- Hegge AB, Vukicevic M, Bruzell E, Kristensen S, Tonnesen HH. Solid dispersions for preparation of phototoxic supersaturated solutions for antimicrobial photodynamic therapy (aPDT): studies on curcumin and curcuminoids L. *Eur J Pharm Biopharm.* 2013;83(1):95-105.
- Li J, Lee IW, Shin GH, Chen X, Park HJ. Curcumin-Eudragit® E PO solid dispersion: a simple and potent method to solve the problems of curcumin. *Eur J Pharm Biopharm.* 2015;94:322-332.
- Kerdsakundee N, Mahattanadul S, Wiwattanapatapee R. Development and evaluation of gastroretentive raft forming systems incorporating curcumin-Eudragit® EPO solid dispersions for gastric ulcer treatment. *Eur J Pharm Biopharm.* 2015;94:513-520.
- Seo S-W, Han H-K, Chun M-K, Choi H-K. Preparation and pharmacokinetic evaluation of curcumin solid dispersion using Solutol® HS15 as a carrier. *Int J Pharm.* 2012;424(1-2):18-25.
- Li B, Konecke S, Wegiel LA, Taylor LS, Edgar KJ. Both solubility and chemical stability of curcumin are enhanced by solid dispersion in cellulose derivative matrices. *Carbohydr Polym.* 2013;98:1108-1116.
- Wegiel LA, Zhao Y, Mauer LJ, Edgar KJ, Taylor LS. Curcumin amorphous solid dispersions: the influence of intra and intermolecular bonding on physical stability. *Pharm Dev Technol.* 2014;19(8):976-986.
- Gangurde AB, Kundaikar HS, Javeer SD, Jaiswar DR, Degani MS, Amin PD. Enhanced solubility and dissolution of curcumin by a hydrophilic polymer solid dispersion and its *in silico* molecular modeling studies. *J Drug Deliv Sci Technol.* 2015;29:226-237.
- Paradkar A, Ambike AA, Jadhav BK, Mahadik KR. Characterization of curcumin–PVP solid dispersion obtained by spray drying. *Int J Pharm.* 2004;271(1-2):281-286.
- Van Duong T, Van den Mooter G. The role of the carrier in the formulation of pharmaceutical solid dispersions. Part I: crystalline and semi-crystalline carriers. *Expert Opin Drug Deliv.* 2016;13(11):1583-1594.
- Van Duong T, Van den Mooter G. The role of the carrier in the formulation of pharmaceutical solid dispersions. Part II: amorphous carriers. *Expert Opin Drug Deliv.* 2016;13(12):1681-1694.
- Kojima T, Higashi K, Suzuki T, Tomono K, Moribe K, Yamamoto K. Stabilization of a supersaturated solution of mefenamic acid from a solid dispersion with EUDRAGIT® EPO. *Pharm Res.* 2012;29(10):2777-2791.
- Xie T, Taylor LS. Dissolution performance of high drug loading celecoxib amorphous solid dispersions formulated with polymer combinations. *Pharm Res.* 2016;33:739-750.
- Liu X, Quan P, Li S, et al. Time dependence of the enhancement effect of chemical enhancers: molecular mechanisms of enhancing kinetics. *J Control Release.* 2017;248:33-44.
- Li J, Guo Y. Basic evaluation of typical nanoporous silica nanoparticles in being drug carrier: structure, wettability and hemolysis. *Mater Sci Eng C Mater Biol Appl.* 2017;73:670-673.

15. Nie H, Liu Z, Marks BC, Taylor LS, Byrn SR, Marsac PJ. Analytical approaches to investigate salt disproportionation in tablet matrices by Raman spectroscopy and Raman mapping. *J Pharm Biomed Anal.* 2016;118:328-337.
16. Li J, Wang X, Li C, et al. Viewing molecular and interface interactions of curcumin amorphous solid dispersions for comprehending dissolution mechanisms. *Mol Pharm.* 2017;14:2781-2792.
17. Sun M, Wu C, Fu Q, et al. Solvent-shift strategy to identify suitable polymers to inhibit humidity-induced solid-state crystallization of lacidipine amorphous solid dispersions. *Int J Pharm.* 2016;503(1-2):238-246.
18. Song W, Quan P, Li S, et al. Probing the role of chemical enhancers in facilitating drug release from patches: mechanistic insights based on FT-IR spectroscopy, molecular modeling and thermal analysis. *J Control Release.* 2016;227:13-22.
19. Zhou FZ, Zhu F, Li J, Wang Y. Concealed body mesoporous silica nanoparticles for orally delivering indometacin with chiral recognition function. *Mater Sci Eng C Mater Biol Appl.* 2018;90:314-324.
20. Li B, Konecke S, Harich K, Wegiel L, Taylor LS, Edgar KJ. Solid dispersion of quercetin in cellulose derivative matrices influences both solubility and stability. *Carbohydr Polym.* 2013;92(2):2033-2040.
21. Xie T, Taylor LS. Improved release of celecoxib from high drug loading amorphous solid dispersions formulated with polyacrylic acid and cellulose derivatives. *Mol Pharm.* 2016;13(3):873-884.
22. Mishra DK, Dhote V, Bhargava A, Jain DK, Mishra PK. Amorphous solid dispersion technique for improved drug delivery: basics to clinical applications. *Drug Deliv Transl Res.* 2015;5(6):552-565.
23. Craig DQM. The mechanisms of drug release from solid dispersions in water-soluble polymers. *Int J Pharm.* 2002;231(2):131-144.
24. Li J, Fan N, Li C, Wang J, Li S, He Z. The tracking of interfacial interaction of amorphous solid dispersions formed by water-soluble polymer and nitrendipine. *Appl Surf Sci.* 2017;420:136-144.
25. He Y, Ho C. Amorphous solid dispersions: utilization and challenges in drug discovery and development. *J Pharm Sci.* 2015;104(10):3237-3258.